



OPEN ACCESS

EDITED BY

Somasundaram Arumugam,
National Institute of Pharmaceutical Education
and Research, Kolkata, India

REVIEWED BY

Weicheng Hu,
Yangzhou University, China
Laiba Arshad,
Forman Christian College, Pakistan
Xican Li,
Guangzhou University of Chinese Medicine,
China

*CORRESPONDENCE

Sanghyun Lee,
✉ slee@cau.ac.kr
Ik-Hyun Cho,
✉ ihcho@khu.ac.kr

RECEIVED 25 March 2024

ACCEPTED 14 August 2024

PUBLISHED 28 August 2024

CITATION

Lee H-D, Kim JH, Choi JH, Kim KH, Ku J, Choi K,
Kim HY, Lee S and Cho I-H (2024) Exploring
phytochemicals and pharmacological
properties of *Populus x tomentiglandulosa*.
Front. Pharmacol. 15:1406623.
doi: 10.3389/fphar.2024.1406623

COPYRIGHT

© 2024 Lee, Kim, Choi, Kim, Ku, Choi, Kim, Lee
and Cho. This is an open-access article
distributed under the terms of the [Creative
Commons Attribution License \(CC BY\)](https://creativecommons.org/licenses/by/4.0/). The use,
distribution or reproduction in other forums is
permitted, provided the original author(s) and
the copyright owner(s) are credited and that the
original publication in this journal is cited, in
accordance with accepted academic practice.
No use, distribution or reproduction is
permitted which does not comply with these
terms.

Exploring phytochemicals and pharmacological properties of *Populus x tomentiglandulosa*

Hak-Dong Lee^{1,2}, Ji Hyun Kim³, Jong Hee Choi⁴, Ki Hyun Kim⁵,
Jajung Ku⁶, Kyung Choi⁷, Hyun Young Kim³, Sanghyun Lee^{1,2*}
and Ik-Hyun Cho^{4*}

¹Department of Plant Science and Technology, Chung-Ang University, Anseong, Republic of Korea, ²Natural Product Institute of Science and Technology, Anseong, Republic of Korea, ³Department of Food Science, Gyeongsang National University, Jinju, Republic of Korea, ⁴Department of Convergence Medical Science, College of Korean Medicine, Kyung Hee University, Seoul, Republic of Korea, ⁵School of Pharmacy, Sungkyunkwan University, Suwon, Republic of Korea, ⁶Department of Forest Bioresources, National Institute of Forest Science, Suwon, Republic of Korea, ⁷Garden and Plant Resources Division, Korea National Arboretum, Pocheon, Republic of Korea

Populus x tomentiglandulosa (PT), a tree endemic to Korea, shows promising potential as a natural therapeutic agent owing to its potent anti-inflammatory properties. However, the isolation and analysis of phytochemical compounds in PT and related species remains underexplored. Therefore, this study aims to investigate the biochemical profile of PT and evaluate its extracts and fractions for anti-inflammatory activities. Nine compounds were isolated, including two novel flavonoids (luteolin 7-O- β -D-glucuronide butyl ester and chrysoeriol 7-O- β -D-glucuronide butyl ester) from the Salicaceae family for the first time. The ethyl acetate fraction exhibited significant radical scavenging activity against various radicals, including DPPH, ABTS⁺, \cdot OH, and O₂⁻ radicals. PT extracts and the ethyl acetate fraction showed minimal cytotoxicity in Raw 264.7 macrophages at concentrations below 500 and 100 μ g/mL, respectively. Furthermore, PT extracts and fractions significantly suppressed the protein expression of proinflammatory mediators (iNOS and IL-6) in LPS-stimulated Raw 264.7 macrophages, highlighting their potent anti-inflammatory effects. These findings suggest that PT holds promise as a valuable natural therapeutic intervention for various oxidative stress and inflammation-related disorders, underscoring the need for further exploration of its clinical applications.

KEYWORDS

Populus x tomentiglandulosa, biochemical profiling, free radical, anti-inflammation, phytomedicine

1 Introduction

The term “reactive oxygen species” (ROS) includes oxygen free radicals such as the superoxide anion radical (O₂⁻), singlet oxygen (¹O₂), hydroxyl radical (OH \cdot), and perhydroxyl radical (HO₂ \cdot) (Phaniendra et al., 2015). ROS are naturally and continually generated through physiological processes in the human body. Free radicals have beneficial effects when present in appropriate or low concentrations, serving various physiological roles, including in cellular signaling pathways and immune responses. However, excessive production of free radicals can induce oxidative stress and impair cell function, leading to various inflammatory, autoimmune, and degenerative diseases (Di Domenico et al., 2014;

Habib and Ibrahim, 2011). Consequently, organisms require endogenous and exogenous antioxidants to reduce oxidative stress (Liu et al., 2017). Synthetic nutritional supplements, classified as artificial exogenous antioxidants, are extensively used in the health functional food industry. However, rising living standards and increasing interest in individual healthcare have sparked a general desire to replace synthetic supplements with natural alternatives (Brown, 2016). Several studies indicate that plant-derived phenolic metabolites enhance their antioxidant ability (Kosseva and Webb, 2013; Lee et al., 2021b; Liu et al., 2021). Plant phenols are used for various purposes, primarily as reducing agents to counteract free radicals, and are present in all plant parts, including leaves, fruits, nuts, roots, bark, and seeds (Guleria et al., 2021; Nam et al., 2017).

The genus *Populus*, which includes poplars and belongs to the Salicaceae family, is predominantly distributed in temperate and subtropical regions. *Populus* spp. are deciduous trees that thrive in dry areas and propagate well from their roots owing to their shallow-rooted characteristics (Choi et al., 2020). These trees are primarily used for fast-growing plantation forestry, particularly in northern regions. They are a crucial fiber resource for the global pulp and paper industry owing to their high growth rates and favorable pulp properties (Greenwood Resources, 2014; Lu et al., 2006). Additionally, they possess significant medicinal value, containing high concentrations of salicylate-like phenolic glycosides and flavonoids. These salicylate-like phenolic glycosides are essential secondary metabolites in the genus *Populus* trees and other species within the Salicaceae family (Abreu et al., 2011). Salicylate compounds function as chemotaxonomic markers and chemical defenses against biotic stressors (Gondor et al., 2022; Khan et al., 2015). After ingestion, salicin is hydrolyzed and oxidized into salicylic acid, which acts similarly to aspirin (Mahdi et al., 2006). Additionally, various flavonoids, including (+)-catechin, eriodictyol, quercetin, kaempferol, pinobanksin, galangin, apigenin, luteolin, and myricetin are isolated from *Populus* spp. (Yang et al., 2023; Morreel et al., 2006; Tsai et al., 2006). Flavonoids are representative plant secondary metabolites with strong antioxidant properties (Zeng et al., 2013). Therefore, several *Populus* spp. have been used in traditional medicine since ancient times (Andelković et al., 2017). *Populus nigra* and *P. tremula* var. *dauriana* exhibit pharmacological properties, including antioxidant, anti-inflammatory, and hepatoprotective effects (Debbache-Benaidat et al., 2013; Zhang et al., 2006). Furthermore, *Populus balsamifera* shows pharmacological potential in treating obesity and diabetes and exhibits antibacterial properties (Harbilas et al., 2012; Simard et al., 2014). Currently, pharmacological companies extensively explore the pharmacological benefits of *Populus* spp.

Among *Populus* species, *P. × tomentiglandulosa* T.B.Lee (PT), known as “Silver aspen” was first reported as a natural hybrid between *P. alba* L. and *P. tremula* var. *glandulosa* Uyeki. Currently, this taxon is recognized as a Korean endemic plant (Chung et al., 2017). Although an artificial hybrid between the two species was made by Dr. S. G. Hyun, since a taxonomic treatment of this natural hybrid was already done (Son, 2009), we will be used this name, *P. × tomentiglandulosa* in this paper. Owing to its rapid growth, PT has been artificially hybridized and extensively used for afforestation and as street trees in South Korea. Numerous studies have reported the phytochemical metabolites and

pharmacological activities of PT, highlighting its significant neuroprotective properties (Choi et al., 2020; Kwon and Koh, 2020; Lee et al., 2019a; Lee et al., 2019b; Park et al., 2017). Nevertheless, the isolation and analysis of phytochemical metabolites in PT and related species remain underexplored.

Therefore, this study aims to investigate various phytochemical constituents of PT leaves and stems using column chromatography, elucidate their structures through spectral analyses, and compare these metabolites with those of their parent species. In addition, we investigated the chemical profiling of PT and four fractions by assessing their radical scavenging activities. Additionally, anti-inflammatory properties of PT extracts and four fractions were demonstrated using lipopolysaccharide-induced Raw 264.7 macrophages.

2 Materials and methods

2.1 Plant materials

Dried PT leaves used for column chromatography were provided by the National Institute of Forest Science, Korea, in February 2020. The stems and leaves of PT, *P. alba*, and *P. tremula* var. *glandulosa* used for High-Performance Liquid Chromatography (HPLC) analysis and bioactivity assays were supplied by the National Institute of Forest Science, Korea, in July 2021. The individuals used in the analysis were planted in an experimental nursery at the National Institute of Forest Science, Suwon, Korea, and the plant specimens used were deposited in the Herbarium (KH) of Korea National Arboretum (Voucher number: No. KH20-10), Pocheon, Korea.

2.2 Apparatuses and chemicals

¹H-nuclear magnetic resonance (NMR) and ¹³C-NMR spectra, heteronuclear single quantum coherence spectroscopy (HSQC), and heteronuclear multiple bond correlation (HMBC) spectra were recorded using an AVANCE III HD 500 NMR spectrometer (Bruker, Hanau, Germany). The spectrometer operated at 500 and 125 MHz for ¹H-NMR and ¹³C-NMR, respectively, and was equipped with a 5 mm BBFO (plus) probehead. Tetramethylsilane served as the internal standard. Fast atom bombardment mass spectrometry (FAB-MS) spectra were recorded using an MS-700 mass spectrometer (JEOL, Japan). Silica gel (60–200 mesh, Zeochem, Switzerland) and Sephadex LH-20 (Sigma-Aldrich, St. Louis, MO, United States) were used as stationary phases for open-column chromatography. Chromatographic separations were monitored using thin-layer chromatography (TLC) with pre-coated Kiesel gel 60 F₂₅₄ plates (silica gel, 0.25 mm layer thickness, Art. 5715, Merck Co., Darmstadt, Germany). Compounds on TLC plates were visualized by spraying them with 10% H₂SO₄ in methanol (MeOH), followed by heating at 100°C on a hot plate. Solvents, including chloroform (CHCl₃), ethyl acetate (EtOAc), *n*-butanol (*n*-BuOH), and MeOH, were purchased from Samchun Pure Chemicals (Pyeongtaek, Republic of Korea). HPLC-grade solvents such as water (H₂O), MeOH, and acetonitrile (ACN) were obtained

from J.T. Baker (Phillipsburg, PA, United States). The compound 1,1-Diphenyl-2-picrylhydrazyl (DPPH) was purchased from Alfa Aesar (London, United Kingdom), while 2,2'-azino-bis(3-ethylbenzothiazoline-6-sulfonic acid (ABTS⁺) was purchased from Roche (Mannheim, Germany). Phenazine methosulfate (PMS), nicotinamide adenine dinucleotide (NADH) disodium salt, nitroterazolium blue chloride (NBT), and thiobarbituric acid (TBA) were purchased from Sigma-Aldrich. Trichloroacetic acid (TCA) was purchased from Samchun Pure Chemicals. Absorbance readings were measured using a GloMax microplate reader (Madison, WI, United States).

2.3 Extraction, fractionation, and isolation procedures

The shade-dried, ground PT (956.4 g) was extracted with ethanol (EtOH, 8 L) under reflux at 83°C–84°C for 3 h, repeated five times. After extraction, the solvent was filtered through filter paper. It was then concentrated using a rotary evaporator (Eyela, Tokyo, Japan) at 55°C, yielding EtOH extracts (232.2 g). Subsequently, the extract was suspended with distilled water and sequentially partitioned with *n*-hexane, CHCl₃, EtOAc, and H₂O-saturated *n*-BuOH. The weights of the fractions obtained were as follows: *n*-hexane (25.1 g), CHCl₃ (14.5 g), EtOAc (16.7 g), and *n*-BuOH (18.9 g). The EtOAc fraction (15 g) was subjected to silica gel column chromatography with a gradient of CHCl₃–MeOH (from 100% CHCl₃ to 100% MeOH), yielding nine subfractions. After TLC examination, fractions 4, 5, 6, and 7 from the first column were combined and loaded onto the Sephadex LH-20 column and gradually eluted with a gradient of H₂O–MeOH (from 5:1 to 1:5) to obtain 12 subfractions. Subfractions 5 and 7 yielded compounds **3** and **2**, respectively. The *n*-BuOH fraction (18 g) was subjected to silica gel column chromatography using a gradient of CHCl₃–MeOH (from 100% CHCl₃ to 100% MeOH), resulting in six subfractions based on TLC experiments. Compounds **1** and **9** were obtained from subfractions 1 and 2, respectively, through MeOH recrystallization. The remaining subfractions were further subjected to column chromatography using Sephadex LH-20. All subfractions were loaded onto the Sephadex LH-20 column and eluted with a gradient of H₂O–MeOH (from 5:1 to 1:5) to purify the compounds. Subfractions 3 and 4 yielded compounds **7** and **8**, respectively, while subfraction 5 yielded compound **6**, and subfraction 6 yielded compounds **4** and **5**.

Compound 1: White powder; FAB-MS *m/z*: 309 [M + Na]⁺; ¹H-NMR (500 MHz, DMSO-*d*₆) δ: 4.76 (1H, d, *J* = 7.5 Hz, Glc-1), 5.08 (1H, d, *J* = 4.5 Hz, H_a-7), 5.35 (1H, d, *J* = 5.0 Hz, H_b-7), 7.00 (1H, dt, *J* = 1.0, 7.5 Hz, H-4), 7.09 (1H, dd, *J* = 1.0, 8.5 Hz, H-6), 7.19 (1H, dt, *J* = 1.5, 7.9 Hz, H-5), 7.35 (1H, dd, *J* = 1.5, 7.5 Hz, H-3). ¹³C-NMR (125 MHz, DMSO-*d*₆) δ: 154.7 (C-1), 131.5 (C-2), 127.2 (C-3), 121.8 (C-4), 127.7 (C-5), 114.8 (C-6), 58.28 (C-7), 101.4 (Glc C-1), 73.4 (Glc C-2), 76.5 (Glc C-3), 69.8 (Glc C-4), 77.1 (Glc C-5), 60.8 (Glc C-6).

Compound 2: White powder; FAB-MS *m/z*: 429 [M + Na]⁺; ¹H-NMR (500 MHz, DMSO-*d*₆) δ: 4.65 (1H, d, *J* = 7.5 Hz, Glc-1), 5.39 (2H, s, H-7), 6.68 (1H, dd, *J* = 3.0, 9.0 Hz, H-4), 6.80 (1H, d, *J* = 3.0, H-6), 7.04 (1H, d, *J* = 9.0 Hz, H-3), 7.52 (2H, br t, *J* = 7.8 Hz, H-3', 5'), 7.68 (1H, br t, *J* = 7.5 Hz, H-4'), 8.02 (2H, dd, *J* = 1.3, 8.3 Hz,

H-2', 6'). ¹³C-NMR (125 MHz, DMSO-*d*₆) δ: 126.7 (C-1), 147.9 (C-2), 117.8 (C-3), 114.6 (C-4), 152.4 (C-5), 115.3 (C-6), 61.7 (C-7), 129.8 (C-1'), 129.3 (C-2'), 128.9 (C-3'), 133.5 (C-4'), 128.9 (C-5'), 129.3 (C-6'), 165.7 (C-7'), 102.7 (Glc C-1), 73.5 (Glc C-2), 77.1 (Glc C-3), 69.9 (Glc C-4), 76.6 (Glc C-5), 60.9 (Glc C-6).

Compound 3: White powder; FAB-MS *m/z*: 413 [M + Na]⁺; ¹H-NMR (500 MHz, DMSO-*d*₆) δ: 5.24 (1H, d, *J* = 8.0 Hz, Glc-1), 5.34 (1H, d, *J* = 5.0 Hz, H_a-7), 5.49 (1H, d, *J* = 5.5 Hz, H_b-7), 6.98 (1H, dt, *J* = 1.0, 7.4 Hz, H-4), 7.08 (1H, dd, *J* = 1.0, 8.5, H-6), 7.17 (1H, dt, *J* = 1.5, 7.8 Hz, H-5), 7.31 (1H, dd, *J* = 2.0, 7.5 Hz, H-3), 7.52 (2H, br t, *J* = 7.8 Hz, H-3', 4'), 7.65 (1H, br t, *J* = 7.3 Hz, H-4'), 7.99 (2H, dd, *J* = 1.5, 8.5 Hz, H-2', 6'). ¹³C-NMR (125 MHz, DMSO-*d*₆) δ: 153.4 (C-1), 131.1 (C-2), 127.3 (C-3), 121.9 (C-4), 126.3 (C-5), 113.9 (C-6), 57.2 (C-7), 129.8 (C-1'), 129.3 (C-2'), 128.7 (C-3'), 133.3 (C-4'), 128.7 (C-5'), 129.3 (C-6'), 165.0 (C-7'), 98.2 (Glc C-1), 73.8 (Glc C-2), 77.2 (Glc C-3), 69.9 (Glc C-4), 74.2 (Glc C-5), 60.5 (Glc C-6).

Compound 4: Yellow powder; FAB-MS *m/z*: 463 [M + H]⁺; ¹H-NMR (500 MHz, DMSO-*d*₆) δ: 3.89 (3H, s, OCH₃), 5.06 (1H, d, *J* = 7.0 Hz, Glc-1), 6.45 (1H, d, *J* = 2.0 Hz, H-6), 6.87 (1H, d, *J* = 2.5 Hz, H-8), 6.94 (1H, d, *J* = 8.0 Hz, H-5'), 6.99 (1H, s, H-3), 7.60 (1H, s, H-2'), 7.59 (1H, dd, *J* = 2.0, 9.0 Hz, H-6'), 12.97 (1H, s, 5-OH). ¹³C-NMR (125 MHz, DMSO-*d*₆) δ: 164.2 (C-2), 103.1 (C-3), 182.1 (C-4), 161.1 (C-5), 99.5 (C-6), 163.0 (C-7), 95.0 (C-8), 156.9 (C-9), 105.3 (C-10), 121.2 (C-1'), 110.3 (C-2'), 148.1 (C-3'), 151.2 (C-4'), 115.8 (C-5'), 120.6 (C-6'), 99.9 (Glc C-1), 73.1 (Glc C-2), 76.4 (Glc C-3), 69.6 (Glc C-4), 77.2 (Glc C-5), 60.6 (Glc C-6), 56.0 (3'-OCH₃).

Compound 5: Yellow powder; FAB-MS *m/z*: 449 [M + H]⁺; ¹H-NMR (500 MHz, DMSO-*d*₆) δ: 5.07 (1H, d, *J* = 7.5 Hz, Glc-1), 6.43 (1H, s, H-6), 6.71 (1H, s, H-3), 6.78 (1H, s, H-8), 6.85 (1H, d, *J* = 8.5 Hz, H-5'), 7.40 (1H, d, *J* = 1.5 Hz, H-2'), 7.43 (1H, dd, *J* = 2.0, 8.5 Hz, H-6'), 13.05 (1H, s, 5-OH). ¹³C-NMR (125 MHz, DMSO-*d*₆) δ: 164.6 (C-2), 102.9 (C-3), 181.8 (C-4), 161.1 (C-5), 99.5 (C-6), 162.9 (C-7), 94.7 (C-8), 156.9 (C-9), 105.3 (C-10), 120.7 (C-1'), 113.2 (C-2'), 146.0 (C-3'), 150.8 (C-4'), 116.0 (C-5'), 119.3 (C-6'), 99.9 (Glc C-1), 73.1 (Glc C-2), 77.2 (Glc C-3), 69.5 (Glc C-4), 76.4 (Glc C-5), 60.6 (Glc C-6).

Compound 6: Yellow powder; FAB-MS *m/z*: 611 [M + H]⁺; ¹H-NMR (500 MHz, DMSO-*d*₆) δ: 0.99 (3H, d, *J* = 6.0 Hz, Rha-CH₃), 4.38 (1H, d, *J* = 1.0 Hz, Rha-1), 5.34 (1H, d, *J* = 7.5 Hz, Glc-1), 6.19 (1H, d, *J* = 2.0 Hz, H-6), 6.38 (1H, d, *J* = 2.0 Hz, H-8), 6.83 (1H, d, *J* = 8.5 Hz, H-5'), 7.52 (1H, d, *J* = 2.0 Hz, H-2'), 7.53 (1H, dd, *J* = 2.3, 10.8 Hz, H-6'), 12.59 (1H, s, 5-OH). ¹³C-NMR (125 MHz, DMSO-*d*₆) δ: 156.5 (C-2), 133.3 (C-3), 177.4 (C-4), 161.2 (C-5), 98.7 (C-6), 164.2 (C-7), 93.6 (C-8), 156.6 (C-9), 103.9 (C-10), 121.6 (C-1'), 115.2 (C-2'), 144.8 (C-3'), 148.5 (C-4'), 116.3 (C-5'), 121.2 (C-6'), 101.2 (Glc C-1), 74.1 (Glc C-2), 76.5 (Glc C-3), 70.0 (Glc C-4), 75.9 (Glc C-5), 67.0 (Glc C-6), 100.8 (Rha C-1), 70.4 (Rha C-2), 70.6 (Rha C-3), 71.9 (Rha C-4), 68.2 (Rha C-5), 17.8 (Rha C-6).

Compound 7: Yellow powder; FAB-MS *m/z*: 625 [M + H]⁺; ¹H-NMR (500 MHz, DMSO-*d*₆) δ: 0.97 (3H, d, *J* = 6.0 Hz, Rha-CH₃), 3.83 (3H, s, OCH₃), 4.41 (1H, d, *J* = 1.0 Hz, Rha-1), 5.43 (1H, d, *J* = 7.5 Hz, Glc-1), 6.20 (1H, d, *J* = 2.0 Hz, H-6), 6.43 (1H, d, *J* = 2.0 Hz, H-8), 6.90 (1H, d, *J* = 8.0 Hz, H-5'), 7.51 (1H, dd, *J* = 2.0, 8.5 Hz, H-6'), 7.85 (1H, d, *J* = 2.5 Hz, H-2'), 12.57 (1H, s, 5-OH). ¹³C-NMR (125 MHz, DMSO-*d*₆) δ: 156.5 (C-2), 133.0 (C-3), 177.3 (C-4), 161.2 (C-5), 98.7 (C-6), 164.2 (C-7), 93.8 (C-8), 156.5 (C-9), 104.0 (C-10), 121.0 (C-1'), 113.3 (C-2'), 146.9 (C-3'), 149.4 (C-4'), 115.2 (C-5'), 122.3 (C-6'), 101.2 (Glc C-1), 74.3 (Glc C-2), 75.9 (Glc

TABLE 1 Calibration curves of compounds 1–9.

Compound	t _R	Calibration equation	Correlation factor, r ²
Salicin (1)	8.4	Y = 732.57X + 12,700	0.9997
Salireposide (2)	31.2	Y = 2176.6X + 44,278	0.9996
Populin (3)	35.0	Y = 2247.3X + 6126	0.9997
Thermopsoside (4)	30.6	Y = 186,61X + 10,228	0.9996
Cynaroside (5)	27.7	Y = 225,27X + 20,287	0.9999
Rutin (6)	26.3	Y = 155,00X + 113,515	0.9994
Narcissin (7)	29.6	Y = 153,78X - 16,025	0.9996
Luteolin 7-O-β-D-glucuronide butyl ester (8)	41.0	Y = 6757X + 1,699.2	0.9999
Chrysoeriol 7-O-β-D-glucuronide butyl ester (9)	44.3	Y = 104,37X + 16,938	0.9994

t_R = retention time. Y = peak area, X = concentration of the standard (μg/mL). r² = correlation coefficient for data points on the calibration curve.

C-3), 70.1 (Glc C-4), 76.4 (Glc C-5), 66.8 (Glc C-6), 100.9 (Rha C-1), 70.3 (Rha C-2), 70.6 (Rha C-3), 71.8 (Rha C-4), 68.3 (Rha C-5), 17.7 (Rha C-6), 55.6 (3'-OCH₃).

Compound 8: Yellow powder; FAB-MS *m/z*: 519 [M + H]⁺; ¹H-NMR (500 MHz, DMSO-*d*₆) δ: 0.83 (3H, t, *J* = 7.5 Hz, H-4'''), 1.32 (2H, m, H-3'''), 1.55 (2H, m, H-2'''), 4.03–4.09 (2H, m, H-1'''), 4.12 (1H, d, *J* = 9.5 Hz, Glc-5), 5.32 (1H, d, *J* = 7.0 Hz, Glc-1), 6.46 (1H, d, *J* = 2.0 Hz, H-6), 6.75 (1H, s, H-3), 6.81 (1H, d, *J* = 2.0 Hz, H-8), 6.89 (1H, d, *J* = 8.0 Hz, H-5'), 7.41 (1H, d, *J* = 2.0 Hz, H-2'), 7.44 (1H, dd, *J* = 2.3, 8.3 Hz, H-6'), 13.01 (1H, s, 5-OH). ¹³C-NMR (125 MHz, DMSO-*d*₆) δ: 168.7 (C-2), 103.0 (C-3), 181.8 (C-4), 162.4 (C-5), 99.1 (C-6), 164.5 (C-7), 94.5 (C-8), 161.1 (C-9), 105.4 (C-10), 121.1 (C-1'), 113.4 (C-2'), 145.9 (C-3'), 150.3 (C-4'), 115.9 (C-5'), 119.1 (C-6'), 99.3 (Glc C-1), 72.7 (Glc C-2), 75.4 (Glc C-3), 71.2 (Glc C-4), 75.1 (Glc C-5), 169.2 (Glc C-6), 64.3 (C-1'''), 30.0 (C-2'''), 18.4 (C-3'''), 13.5 (C-4''').

Compound 9: Yellow powder; FAB-MS *m/z*: 533 [M + H]⁺; ¹H-NMR (500 MHz, DMSO-*d*₆) δ: 0.83 (3H, t, *J* = 7.5 Hz, H-4'''), δ 1.31 (2H, m, H-3'''), δ 1.56 (2H, m, H-2'''), 3.90 (3H, s, OCH₃), 4.03–4.13 (2H, m, H-1'''), 4.18 (1H, d, *J* = 9.5 Hz, Glc-5), 5.31 (1H, d, *J* = 7.0 Hz, Glc-1), 6.48 (1H, d, *J* = 2.5 Hz, H-6), 6.87 (1H, d, *J* = 2.0 Hz, H-8), 6.95 (1H, d, *J* = 9.0 Hz, H-5'), 7.00 (1H, s, H-3), 7.59 (1H, dd, *J* = 2.0, 8.8 Hz, H-6'), 7.60 (1H, d, *J* = 2.0 Hz, H-2'), 12.99 (1H, s, 5-OH). ¹³C-NMR (125 MHz, DMSO-*d*₆) δ: 164.2 (C-2), 103.5 (C-3), 182.1 (C-4), 161.2 (C-5), 99.3 (C-6), 162.4 (C-7), 94.9 (C-8), 156.9 (C-9), 105.5 (C-10), 121.3 (C-1'), 110.4 (C-2'), 148.1 (C-3'), 151.0 (C-4'), 115.8 (C-5'), 120.5 (C-6'), 99.4 (Glc C-1), 72.8 (Glc C-2), 75.5 (Glc C-3), 71.2 (Glc C-4), 75.2 (Glc C-5), 168.7 (Glc C-6), 64.4 (C-1'''), 30.0 (C-2'''), 18.5 (C-3'''), 13.5 (C-4'''), 56.0 (3'-OCH₃).

2.4 Sample preparation for HPLC and HPLC conditions

To quantify compounds 1–9 in each *Populus* spp. extract, 45 mg of each extract was dissolved in 3 mL of MeOH to prepare a stock solution. The resulting solutions were filtered through a Whatman 0.45-μm polyvinylidene difluoride (PVDF) syringe filter (Cat No. 6779, Whatman plc, Maidstone, United Kingdom) before HPLC analysis. A reverse-phase HPLC system with a YMC-Pack Pro

C18 column (25 cm × 4.6 mm, 5 μm) was used for simultaneous analysis of the nine compounds. The injection volume was 10 μL, and detection was monitored at 252 nm. The column oven temperature was maintained at 30°C, while the flow rate was set at 1.0 mL/min. A gradient elution system was used for the analysis. The mobile phase consisted of 0.25% acetic acid in water (A) and ACN (B). Elution gradient was conducted as follows: 90% A at 0 min and maintained until 10 min; 80% A from 10 to 20 min; 70% A from 20 to 30 min; 50% A from 30 to 45 min; 0% A from 45 to 50 min and maintained until 55 min; and 90% A from 55 to 60 min, maintained until 70 min.

2.5 Calibration curves

Standard stock solutions (0.5–1 mg/mL) of compounds 1–9 isolated from PT were prepared in MeOH and repeatedly mixed with the same solvent. The purity of the isolated compounds was determined by HPLC analysis, with all compounds exhibiting a purity of greater than 94%. Calibration curves were plotted by correlating the concentrations of the standard solutions with their respective peak areas. The linearity of the calibration curves was determined using the correlation coefficient (r²). Subsequently, the concentrations of compounds 1–9 in the samples were calculated from the calibration curves. The calibration functions were derived from the peak area (Y) and concentration (X, μg/mL), with results presented as mean ± standard deviation (*n* = 3) (Table 1).

2.6 DPPH radical scavenging activity

DPPH radical scavenging activity was measured as described by Kwon et al. (2020). The extract and four fractions, including the active compounds from PT, were dissolved in EtOH. Subsequently, the samples were mixed with a 60-μM DPPH solution in 96-well plates and incubated in the dark at room temperature. After 30 min, absorbance at 540 nm was measured using a microplate reader. DPPH radical scavenging activity was calculated using the formula: DPPH radical scavenging activity (%) = [(Abs_c - Abs_s)/Abs_c] × 100, where Abs_c and Abs_s represent the absorbance of the control and sample, respectively.

2.7 ABTS⁺ radical scavenging activity

ABTS⁺ radical scavenging activity was measured as previously described by [Thaipong et al. \(2006\)](#). The ABTS⁺ solution was prepared by reacting 2,2'-azinobis-(3-ethylbenzothiazolin-6-sulfonic acid) (ABTS, 7.4 mM) with potassium persulfate (2.6 mM) for 12–16 h in the dark until the oxidation-reduction reaction occurred and ABTS⁺ was formed. The working ABTS solution was prepared by diluting the stock solution with purified water until the absorbance reached 1.0 at 600 nm. Subsequently, the fraction samples were mixed with the working ABTS⁺ solution in 96-well plates and incubated in the dark at room temperature. After 30 min, the absorbance at 600 nm was measured using a microplate reader with L-ascorbic acid serving as the positive control. ABTS⁺ radical scavenging activity was calculated using the formula: ABTS⁺ radical scavenging activity (%) = $[(Abs_c - Abs_s)/Abs_c] \times 100$, where Abs_c and Abs_s represent the absorbance of the control and sample, respectively.

2.8 •OH radical scavenging activity

•OH radical scavenging activity was measured using the method described by [Kwon et al. \(2020\)](#). The fractions of PT were evaporated to dryness to remove the solvent ([Li, 2013](#)). Subsequently, four fractions of PT were dissolved in phosphate-buffered saline and mixed with 10 mM FeSO₄•7H₂O-EDTA, 10 mM 2-deoxyribose, and 10 mM H₂O₂. The mixtures were incubated at 37°C in the dark for 4 h. After this, 1% TBA and 2.8% TCA solutions were added, and the mixtures were heated to 100°C for 20 min. After cooling, the absorbance was measured at 490 nm using a microplate reader. L-ascorbic acid was used as the positive control. •OH radical scavenging activity was calculated using the formula: •OH radical scavenging activity (%) = $[(Abs_c - Abs_s)/Abs_c] \times 100$, where Abs_c denotes the absorbance of the control, and Abs_s denotes the absorbance of the sample.

2.9 O₂⁻ radical scavenging activity

O₂⁻ radical scavenging activity was assessed following the method described by [Kwon \(2020\)](#). Four fractions of PT diluted in H₂O were mixed with 0.1 M Tris-HCl (pH 7.4), 200 μM PMS, 1 mM NBT, and 1 mM NADH and incubated at room temperature in the dark. After 10 min, absorbance was measured at 560 nm using a microplate reader. L-ascorbic acid was used as the positive control. O₂⁻ radical scavenging activity was calculated using the formula: O₂⁻ radical scavenging activity (%) = $[(Abs_c - Abs_s)/Abs_c] \times 100$, where Abs_c denotes the absorbance of the control, and Abs_s denotes the absorbance of the sample.

2.10 Cell viability assay using MTT assay

The murine macrophage cell line, RAW 264.7, was purchased from the Korean Cell Line Bank (Seoul, Republic of Korea). The cells were cultured in Dulbecco's Modified Eagle Medium (DMEM; Gibco, Paisley, United Kingdom) supplemented with 10% fetal bovine serum (FBS; Gibco) and 1% penicillin/streptomycin (Gibco) and incubated at 37°C in a 5% CO₂ atmosphere. The 3-(4,5-dimethylthiazol-2-yl)-2,5-diphenyl tetrazolium bromide (MTT) assay was used to assess

cellular metabolic activity as an indicator of cell viability, proliferation, and cytotoxicity. RAW 264.7 cells (1×10^4 cells/well) were seeded in 96-well plates and incubated for 24 h. Subsequently, the cells were exposed to various concentrations (0.01–1,000 μg/mL) of samples for an additional 24 h. MTT solution (0.5 mg/mL, 100 μL) was added to each well, and the cells were further incubated for ~3 h at 37°C. The resulting formazan crystals were dissolved in dimethyl sulfoxide (DMSO; 100 μL), and the absorbance was measured at 570 nm using a microplate reader (Molecular Devices Filter Max F5; San Francisco, CA, United States).

2.11 Evaluation of anti-inflammatory effects using western blot analysis

The Raw 264.7 cells were seeded into 6-well plates at a density of 5×10^5 cells/well. After 18 h, the cells were exposed to PT fractions at various concentrations (0.1–100 μg/mL) at 1 h before stimulation with lipopolysaccharides (0127:B8; 1 μg/mL; Sigma-Aldrich). After 5 h of lipopolysaccharide treatment, the cells were collected for Western blot analysis. The Western blot assay was conducted following previously described methods ([Choi et al., 2021a](#); [Choi et al., 2021b](#); [Jang et al., 2019](#); [Lee et al., 2021a](#)). Briefly, the Raw 264.7 cells were homogenized in a cell lysis buffer containing 10 mM Tris-Cl (pH 7.4), 0.5 mM ethylenediaminetetraacetic acid, 0.25 M sucrose, and a protease inhibitor mixture using a bullet blender tissue homogenizer (Next Advance, Inc., Troy, NY, United States). The Western blot assay, protein transfer to PVDF membranes, and membrane blocking were conducted following previously described methods ([Choi et al., 2021a](#); [Choi et al., 2021b](#); [Jang et al., 2019](#); [Lee et al., 2021a](#)). The PVDF membranes were incubated with primary antibodies, including rat anti-interleukin (IL)-6 (1:500, Cell Signaling Technology, Danvers, MA, United States), rat anti-inducible nitric oxide (1:500, Cell Signaling Technology), and rabbit anti-GAPDH (Cell Signaling Technology), followed by incubation with horseradish peroxidase-conjugated secondary antibody (1:500, Vector Laboratories, Newark, CA, United States). Blot signals were detected using an enhanced chemiluminescence kit (Merck KGaA, Darmstadt, Germany). Each Western blot analysis was conducted in triplicate and independently repeated three times, yielding consistent results. Protein band density was measured using ImageJ software.

2.12 Statistical analysis

All results were presented as mean ± SD. Statistical significance ($p < 0.05$) was determined using analysis of variance (ANOVA) followed by Duncan's multiple range tests or Tukey's *post hoc* test using the Statistical Package for the Social Sciences (SPSS, Chicago, IL, United States).

3 Results and discussion

3.1 Identification of phytochemical compounds in PT extract

The EtOAc- and *n*-BuOH-soluble fractions of PT were chromatographically separated, leading to the isolation of

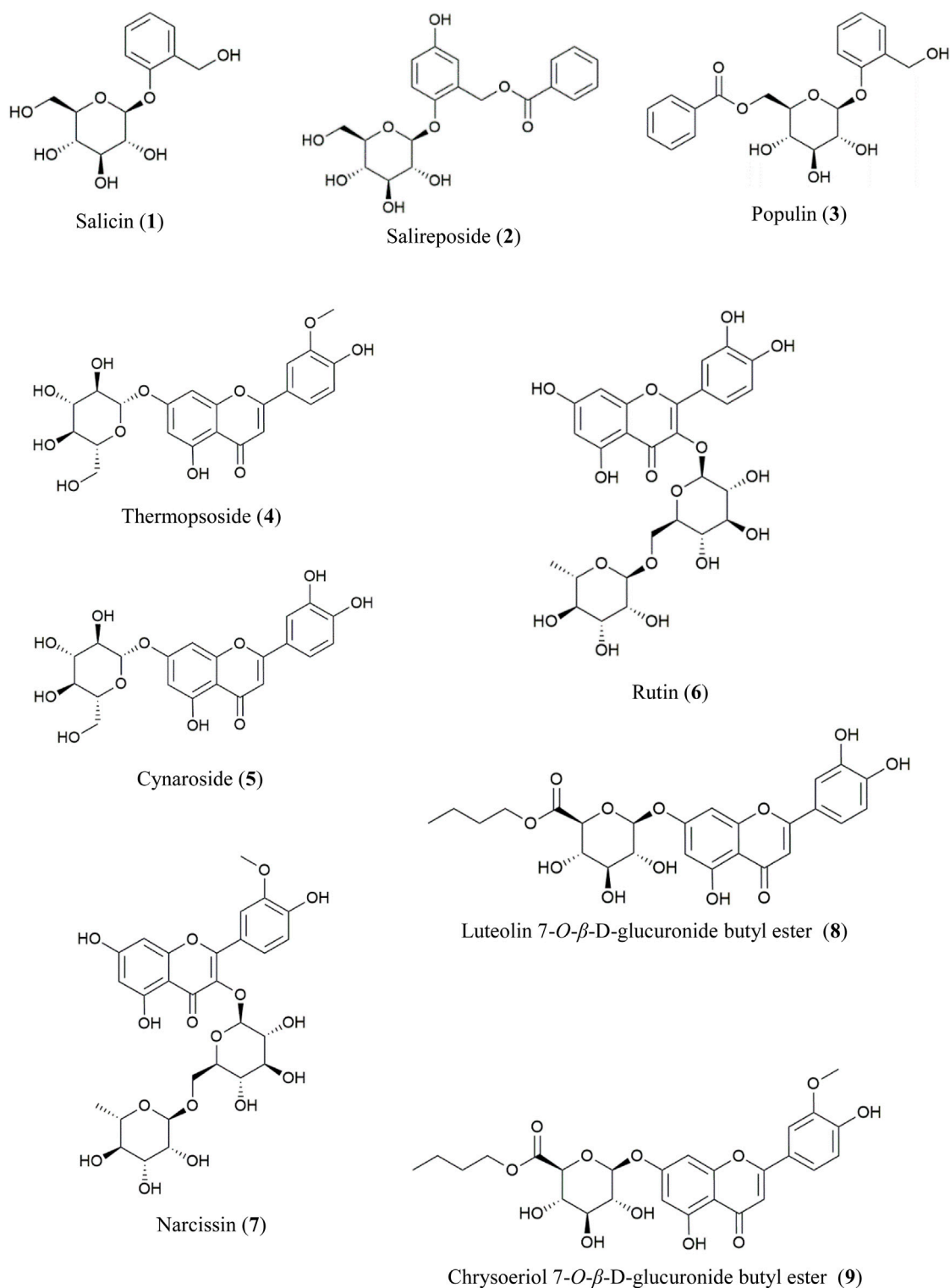


FIGURE 1
Chemical structures of compounds 1–9 from PT.

compounds 1–9 through repeated column chromatography. Their structures were elucidated using spectroscopic analysis and comparison with literature values (Figure 1).

From the EtOAc-soluble fraction, three salicylate-like phenolic compounds were isolated. Compounds 1–3 were obtained as white

powders. Compound 1 exhibited a molecular ion peak at m/z 309 $[M + Na]^+$ in the FAB-MS, corresponding to the molecular formula $C_{13}H_{18}O_7$. Compound 2 displayed a molecular ion peak at m/z 429 $[M + Na]^+$ in the FAB-MS, corresponding to the molecular formula $C_{20}H_{22}O_9$, while compound 3 showed a molecular ion peak

at m/z 413 $[M + Na]^+$ in the FAB-MS, corresponding to the molecular formula $C_{20}H_{22}O_8$. The NMR spectra of compounds **1–3** exhibited characteristic signals with salicylate-like phenolic glycosides. The 1H NMR spectra revealed characteristic signals of a salicyl alcohol unit ranging from δ 6.68 to δ 7.35 and a glucosyl moiety appearing between δ 3.30 and δ 5.24. Only compounds **2** and **3** exhibited benzoyl protons between δ 7.52 and δ 8.02 in their 1H NMR spectra. Compound **2** showed one less hydrogen integral than compound **3** in the downfield region of the 1H NMR spectrum, attributable to the presence of gentisyl alcohol (5-OH) in compound **2** and salicyl alcohol (4-H) in compound **3**. Based on the ^{13}C -NMR spectra, compounds **2** and **3** with a benzoyl group displayed seven carbon peaks ranging from δ 128.7 to δ 165.7. The peaks at δ 165.0 and δ 165.7 corresponded to the ester linkage between benzoic acid and a sugar unit. Additionally, in the spectra of compounds **1–3**, peaks corresponding to the glucosyl moiety were observed between δ 60.5 and δ 77.2, with the anomeric carbon appearing at δ 101.4, δ 102.7, and δ 98.2, respectively. Among the carbons associated with salicyl alcohol, C-7 was observed in the upfield region around δ 57.2– δ 61.7, while the remaining carbons were detected between δ 113.9 and δ 154.7. Since compound **2** has a gentisyl alcohol structure, C-5 was downfield shifted by a hydroxyl group, appearing at δ 152.4. Consequently, the structures of compounds **1**, **2**, and **3** were identified as salicin, salireposide, and populin, respectively. All acquired spectroscopic data were analyzed and compared with literature values (Ahmad et al., 2003; Kumari et al., 2016; Xu et al., 2018).

Various flavonoid glycosides were isolated from the *n*-BuOH-soluble fraction. In the FAB-MS, all isolated compounds exhibited molecular ion peaks consistent with their corresponding molecular formulas, as described in the Materials and Methods. Typical flavonoid signals were observed in the 1H -NMR spectra of compounds **4–9**. The presence of singlet signals at δ 12.57– δ 13.01 indicated the 5-OH group of the A-ring in the structure. A pair of *meta*-coupled aromatic proton signals (d, $J = 2.0$ – 2.5 Hz) localized at δ 6.19– δ 6.94 corresponded to the H-6 and H-8 protons of the A-ring. Additionally, a *meta*-coupled doublet corresponded to H-2' at δ 7.50– δ 7.85 (1H, d, $J = 2$ – 2.5 Hz), and an *ortho-meta*-coupled doublet-doublet corresponded to H-6' at δ 7.43– δ 7.60 (1H, dd, $J = 2$ – 2.3 , 8– 8.8 Hz). The *ortho*-coupled doublet H-5' at δ 6.83– δ 6.95 (1H, d, $J = 8$ – 8.5 Hz) exhibited ABX splitting signals indicative of the B-ring structure in flavonoids. In compounds **4** and **5**, the anomeric proton signal of the glucosyl moiety was detected at δ 5.06 (1H, d, $J = 7.0$ Hz, Glc-1) and δ 5.07 (1H, d, $J = 7.5$ Hz, Glc-1), respectively. In each ^{13}C -NMR spectrum, a signal at δ 99.9 corresponded to the anomeric carbon of *D*-glucose. Additionally, in the 1H -NMR spectra of compounds **4** and **7**, the methoxy signals were observed at δ 3.89 and δ 3.83, respectively. The downfield shift of the H-2' signal relative to the H-6' signal suggests the presence of a 3'-methoxy-4'-hydroxy moiety in the B-ring. In compounds **6** and **7**, each of the two anomeric protons of sugars were observed at δ 5.34 (1H, d, $J = 7.5$ Hz, Glc-1) and δ 4.38 (1H, d, $J = 1.0$ Hz, Rha-1) and δ 5.43 (1H, d, $J = 7.5$ Hz, Glc-1), δ 4.41 (1H, d, $J = 1.0$ Hz, Rha-1), respectively. Additionally, the rhamnosyl CH_3 signals were observed in the upfield region at δ 0.99 and δ 0.97 (3H, d, $J = 6.0$ Hz) for compounds **6** and **7**, respectively. In the ^{13}C -NMR spectra of compounds **6** and **7**, two peaks at δ 101.2, δ 100.8, and 101.2, δ 100.9, were assignable to the two anomeric carbons of

D-glucose and *L*-rhamnose, respectively. The remaining sugar-related peaks of compound **7** were similar to those of compound **6**, suggesting the presence of the same sugar: rutinose. Based on these interpretations and direct comparisons with published literature, compounds **4**, **5**, **6**, and **7** were identified as thermopsoside (chrysoeriol 7-*O*-glucoside), cynaroside (luteolin 7-*O*-glucoside), rutin (quercetin-3-*O*-rutinoside), and narcissin (isorhamnetin 3-*O*-rutinoside), respectively (Akbari-Ahangar and Delnavazi, 2020; Ilhan et al., 2019; Shojaeifard et al., 2021).

Compound **8** was recrystallized from MeOH as a yellow powder. A molecular ion peak was measured at m/z : 519 $[M + H]^+$ in the FAB-MS (positive mode), suggesting a molecular formula of $C_{25}H_{26}O_{12}$. In the HSQC spectrum, correlations were observed between H-3 (δ 6.75) and C-3 (δ 103.0), H-6 (δ 6.46) and C-6 (δ 99.1), H-8 (δ 6.81) and C-8 (δ 94.5), H-2' (δ 7.41) and C-2' (δ 113.4), H-5' (δ 6.89) and C-5' (δ 115.9), and H-6' (δ 7.44) and C-6' (δ 119.1). These correlations indicate the presence of a 5,7,3',4'-tetrasubstituted flavone (luteolin) in the structure. An anomeric proton signal at δ 5.32 (1H, d, $J = 7.0$ Hz, H-1'') showed an HSQC correlation with the corresponding anomeric carbon at δ 99.3 (C-1''). The sugar moiety was identified as glucuronic acid through additional characteristic signals of glucuronic acid [δ 4.12 (1H, d, $J = 9.5$ Hz, H-5''), δ 169.2 (C-6'')]. The β -configuration and *D*-configuration were deduced from the coupling constant of 7.0 Hz (Ashenurst, 2022) and literature (Nzowa et al., 2010), respectively. Additionally, each proton signal appearing at δ 4.03–4.09 (2H, m, H-1'''), δ 1.55 (2H, m, H-2'''), δ 1.32 (2H, m, H-3'''), δ 0.83 (3H, t, $J = 7.5$ Hz, H-4''') showed HSQC correlations with the carbon signals at δ 64.3 (C-1'''), δ 30.0 (C-2'''), δ 18.4 (C-3'''), and δ 13.5 (C-4'''), respectively. This corresponds to a butyl group composed of three methylene and one methyl group. The connectivity of the luteolin aglycone, glucuronic acid moiety, and butyl ester group was established through HMBC correlations. Correlations were specifically observed between the anomeric proton at δ 5.32 (H-1'') and carbon signal at δ 164.5 (C-7), indicating their spatial proximity. Additionally, correlations were observed between the oxymethylene protons of the butyl ester group at δ 4.03–4.09 (H-1''') and the carbonyl carbon of the glucuronic acid moiety at δ 169.2 (C-6''), confirming their structural connectivity. Based on the data explained above and comparisons with spectral data from previously reported values (Shi-hui, 2012), the structure of compound **8** was identified as luteolin 7-*O*- β -*D*-glucuronide butyl ester.

Compound **9** was recrystallized from MeOH, resulting in a yellow powder. The FAB-MS (positive mode) showed a molecular ion peak at m/z : 533 $[M + H]^+$, suggesting a molecular formula of $C_{25}H_{28}O_{13}$. The 1H and ^{13}C -NMR spectra closely resembled those of compound **8**, with significant differences. In the 1H -NMR spectrum, a prominent singlet was observed at δ 3.90 (3H, s), indicative of a methoxy group, which was also observed in the ^{13}C -NMR at δ 56.0. Furthermore, the HMBC correlation between the methoxy group at δ 3.90 (OCH₃) and the carbon signal at δ 148.1 (C-3') confirmed the presence of a 3'-methoxy in the flavonoid B ring. Additionally, the HMBC correlations showed the anomeric proton at δ 5.31 (H-1'') connected to the carbon signal at δ 162.4 (C-7) and the oxymethylene protons of the butyl ester group at δ 4.03–4.13 (H-1''') connected to the carbonyl carbon of the glucuronic acid moiety at δ 168.7 (C-6''), as observed in compound **8**. By comparing these

TABLE 2 Compounds 1–9 content in *Populus* species.

Compound	Content (mg/g ext.)					
	Leaves			Stems		
	PT	<i>P. alba</i>	<i>P. tremula</i> var. <i>glandulosa</i>	PT	<i>P. alba</i>	<i>P. tremula</i> var. <i>glandulosa</i>
Salicin (1)	19.50 ± 0.11 ^a	2.02 ± 0.03 ^c	17.88 ± 0.06 ^b	5.84 ± 0.02 ^b	4.98 ± 0.04 ^c	10.23 ± 0.03 ^a
Salireposide (2)	22.92 ± 0.04 ^a	1.82 ± 0.06 ^c	17.30 ± 0.11 ^b	32.43 ± 0.65 ^b	5.11 ± 0.05 ^c	34.67 ± 0.44 ^a
Populin (3)	17.67 ± 0.02 ^a	tr	4.55 ± 0.03 ^b	9.41 ± 0.07 ^a	2.50 ± 0.04 ^c	7.30 ± 0.06 ^b
Thermopsoside (4)	1.27 ± 0.01 ^a	1.11 ± 0.01 ^b	tr	1.86 ± 0.02 ^b	tr	6.00 ± 0.11 ^a
Cynaroside (5)	4.21 ± 0.01 ^b	1.01 ± 0.00 ^c	17.92 ± 0.19 ^a	0.44 ± 0.00 ^a	0.15 ± 0.00 ^b	0.11 ± 0.00 ^c
Rutin (6)	15.10 ± 0.01 ^a	5.12 ± 0.01 ^b	0.32 ± 0.00 ^c	tr	0.52 ± 0.00	tr
Narcissin (7)	11.97 ± 0.01 ^a	7.20 ± 0.05 ^b	1.11 ± 0.01 ^c	1.57 ± 0.02 ^a	0.67 ± 0.01 ^b	0.64 ± 0.00 ^b
Luteolin 7- <i>O</i> -β-D-glucuronide butyl ester (8)	0.97 ± 0.00	ND	ND	0.12 ± 0.00	ND	ND
Chrysoeriol 7- <i>O</i> -β-D-glucuronide butyl ester (9)	1.09 ± 0.00	ND	ND	0.20 ± 0.00 ^b	0.25 ± 0.00 ^a	0.13 ± 0.00 ^c

tr, trace; ND, not detected. Values are means ± SD.

^{a-c}Different letters for the same compound from the same plant part indicate statistically significant differences ($p < 0.05$) according to the Tukey test.

spectra with those of compound 8 and the previously mentioned data, the structure of compound 9 was determined to be chrysoeriol 7-*O*-β-D-glucuronide butyl ester. This structure was further validated by comparison with previously reported values (Wei et al., 2018).

Of the nine isolated compounds, populin (3), thermopsoside (4), cynaroside (5), rutin (6), narcissin (7), luteolin 7-*O*-glucuronide butyl ester (8), and chrysoeriol 7-*O*-glucuronide butyl ester (9) were identified from PT for the first time. Additionally, luteolin 7-*O*-β-D-glucuronide butyl ester (8) and chrysoeriol 7-*O*-β-D-glucuronide butyl ester (9) were identified from the *Populus* genus for the first time.

3.2 HPLC analysis comparing compounds 1–9 content in *Populus* species

HPLC quantitative analysis was performed on PT leaves following chromatographic isolation. To compare plant parts and species, the leaves and stems of *P. alba* and *P. glandulosa*, along with PT, were analyzed (Table 2). Furthermore, an appropriate HPLC method for the simultaneous analysis of the nine isolated compounds was developed. A UV wavelength of 252 nm was employed for the simultaneous analysis of salicylate-like phenolic compounds from the EtOAc fraction and flavonoid glycosides from the *n*-BuOH fraction. The established HPLC method was used to achieve an ideal separation of the peaks of interest (Figure 2). Table 1 presents the retention times for each compound and the correlation coefficient (r^2) values for the linearity of the method. The salicylate-like compounds in PT leaves were generally abundant. Among the six *Populus* samples, salicin (1) and populin (3) showed the highest concentrations in PT leaves (Table 2), while salireposide (2) had the third-highest concentration after the stems of PT and *P. glandulosa*. Additionally, among the flavonoid glycosides, rutin (6) and narcissin (7) were present in significantly higher

concentrations than in other *Populus* species samples. Thermopsoside (4) and cynaroside (5) had the third and second-highest concentrations, respectively, among the six samples. Cynaroside (5) was particularly abundant in the leaves of *P. tremula* var. *glandulosa*.

Luteolin 7-*O*-β-D-glucuronide butyl ester (8) and chrysoeriol 7-*O*-β-D-glucuronide butyl ester (9) were commonly found in the leaves and stems of PT, with higher concentrations in the leaves. However, their levels were lower compared to other isolated compounds, as these compounds are rarely found in plants. Luteolin 7-*O*-β-D-glucuronide butyl ester (8) was not identified in any extracts other than those of PT, and chrysoeriol 7-*O*-β-D-glucuronide butyl ester (9) was identified in little quantities only in the stems of *P. alba* and *P. tremula* var. *glandulosa*. PT, an endemic species in Korea, seems to contain more phenolic and flavonoid glycosides overall than its parent species, *P. alba* and *P. tremula* var. *glandulosa*.

3.3 Radical scavenging activities of the extract and four fractions of PT

Subsequently, we investigated whether the PT extract and its four fractions exhibit radical scavenging activity to evaluate their chemical profiling. The DPPH is a violet-colored, stable free radical with strong absorption in EtOH. When DPPH solution is combined with a chemical that may donate a hydrogen atom, it is transformed to a reduced form, and its color is lost (Kedare and Singh, 2011; Sharma and Bhat, 2009). Table 3 shows that the DPPH radical scavenging activity of the EtOH extract and four fractions of PT was confirmed. The EtOH extract and four fractions of PT exhibited concentration-dependent DPPH radical scavenging activity. The EtOAc PT fraction exhibited DPPH radical scavenging activity of 66.98% ± 2.25% at a concentration of 100 μg/mL. Ascorbic acid, commonly used as a positive control for evaluating chemical

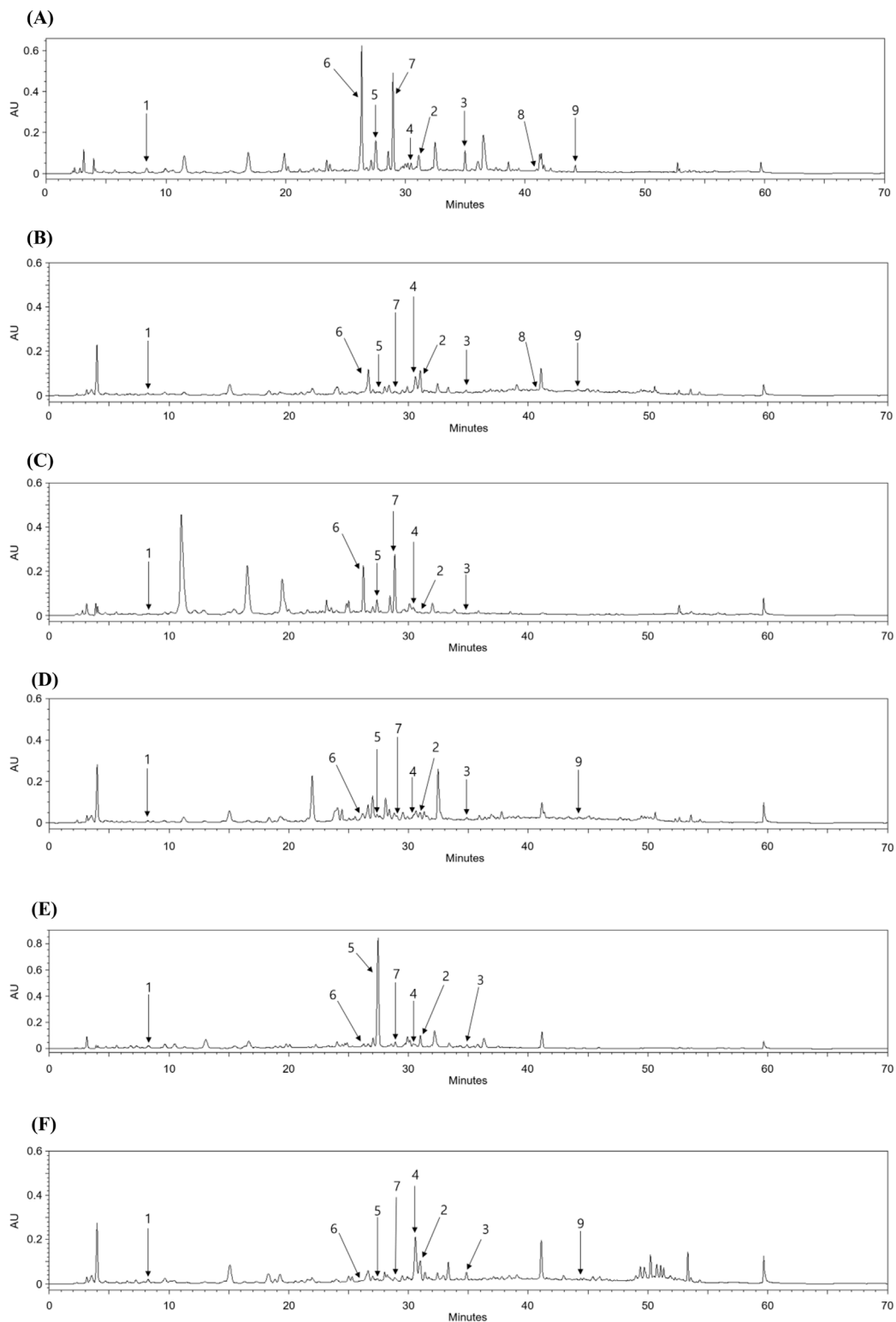


FIGURE 2
HPLC chromatograms of the leaves (A) and stems (B) of PT, leaves (C) and stems (D) of *P. alba*, and leaves (E) and stems (F) of *P. glandulosa*.

profiling, has an IC₅₀ value of 66.12 µg/mL in DPPH radical scavenging activity (Jadid et al., 2017). Among the EtOH extract and four fractions of PT, the EtOAc PT fraction had the lowest IC₅₀ value (58.89 ± 1.51 µg/mL) for DPPH radical scavenging activity.

The characteristic absorbance of ABTS⁺, a protonated radical, is high at 600 nm and decreases when these radicals are scavenged. Incubation of ABTS with potassium persulfate produces ABTS⁺. The presence of chemical compounds in the tested extracts that inhibit

TABLE 3 Radical scavenging activities of PT extracts and fraction.

Scavenging activity	Concentration (µg/mL)	Sample (%)				
		EtOH ext	<i>n</i> -Hexane fr	Chloroform fr	Ethyl acetate fr	<i>n</i> -Butanol fr
DPPH radical	5	0.46 ± 2.26 ^d	-	-	1.07 ± 2.62 ^d	-
	25	10.95 ± 1.18 ^c	2.25 ± 2.68 ^c	1.50 ± 2.26 ^c	23.16 ± 1.61 ^c	11.34 ± 3.06 ^c
	50	18.58 ± 0.80 ^b	9.75 ± 1.58 ^b	5.57 ± 1.25 ^b	42.30 ± 1.03 ^b	22.54 ± 1.96 ^b
	100	30.73 ± 1.32 ^a	16.27 ± 1.01 ^a	15.04 ± 0.94 ^a	66.98 ± 2.25 ^a	41.08 ± 1.48 ^a
ABTS ⁺ radical	5	9.47 ± 1.49 ^d	-	-	7.49 ± 1.16 ^d	1.49 ± 2.20 ^d
	25	20.86 ± 1.57 ^c	-	5.26 ± 0.37 ^c	35.87 ± 1.86 ^c	20.44 ± 1.79 ^c
	50	28.10 ± 2.26 ^b	4.43 ± 1.43 ^b	12.88 ± 0.93 ^b	58.39 ± 1.14 ^b	38.21 ± 1.49 ^b
	100	48.69 ± 1.43 ^a	12.71 ± 0.97 ^a	23.91 ± 0.70 ^a	87.39 ± 1.11 ^a	63.03 ± 1.01 ^a
•OH radical	5	13.66 ± 3.26 ^d	20.80 ± 0.97 ^d	13.91 ± 1.37 ^d	10.09 ± 0.35 ^d	13.28 ± 0.47 ^d
	25	26.09 ± 3.04 ^c	60.55 ± 0.21 ^c	59.09 ± 0.11 ^c	48.03 ± 2.97 ^c	54.14 ± 0.19 ^c
	50	38.82 ± 2.74 ^b	75.00 ± 0.43 ^b	73.40 ± 0.33 ^b	71.49 ± 0.88 ^b	69.69 ± 0.52 ^b
	100	53.73 ± 4.15 ^a	79.15 ± 0.20 ^a	77.50 ± 0.23 ^a	79.63 ± 0.11 ^a	79.57 ± 0.24 ^a
O ₂ ⁻ radical	5	-	5.30 ± 0.58 ^{NS}	9.17 ± 0.92	8.00 ± 2.29 ^c	6.49 ± 1.23 ^{NS}
	25	-	-	-	7.12 ± 2.40 ^c	8.10 ± 3.83
	50	19.16 ± 1.33 ^b	1.86 ± 0.77	-	13.42 ± 2.62 ^b	8.94 ± 4.41
	100	26.93 ± 1.87 ^a	4.94 ± 0.61	-	24.79 ± 2.80 ^a	6.04 ± 3.10

Values are presented as means ± SD, fr, fraction. ^{a-d}Means are significantly different (*p* < 0.05) based on Duncan’s multiple range test.

potassium persulfate activity may reduce ABTS⁺ production (Hernández-Rodríguez et al., 2019). Table 3 presents the efficiency of ABTS⁺ radical scavenging activity at varying sample concentrations. The EtOH extract and four fractions of PT exhibited concentration-dependent ABTS⁺ radical scavenging activity. In this investigation, the EtOAc and *n*-BuOH fractions of PT showed enzymatic inhibition percentages of 87.39% ± 1.11% and 63.03% ± 1.01%, respectively, at a concentration of 100 µg/mL. The results of ABTS⁺ radical scavenging activity reflected a broader range of radical scavenging activity than those of DPPH radical scavenging activity (Table 3), as ABTS⁺ can assess the hydrophilic and hydrophobic samples (Krishnaiah et al., 2011). In previous studies, the IC₅₀ value of ascorbic acid, commonly used as a positive control, was 50 µg/mL in ABTS⁺ radical scavenging activity assessments (Vidya et al., 2016). Among the PT extract and its fractions, the EtOAc fraction exhibited the lowest IC₅₀ value (31.10 ± 0.47 µg/mL) for ABTS⁺ radical scavenging activity.

Photoproduced Fe (II) interacts with H₂O₂ to reduce Fe (III) and generate •OH radicals in the photo-Fenton reaction (Lyngsie et al., 2018). •OH radicals are the most reactive and harmful radicals, implicated in a range of human ailments. They can react vigorously, damaging essential cell components, including mitochondria, DNA, and cell membranes (Lipinski, 2011). Consequently, •OH radicals have been associated with various disorders, including aging, obesity, rheumatoid arthritis, and neurological diseases (Pizzino et al., 2017; Martemucci et al., 2022). Therefore, eliminating •OH radicals provides protection against various ailments. Table 3 shows the •OH radical scavenging activity of the EtOH extract and four fractions of PT. Except for

the extracts, all four fractions exhibited significantly high radical scavenging activity at concentrations of 5, 25, 50, and 100 µg/mL. The EtOAc fractions of PT demonstrated over 90% radical scavenging activity in all concentrations. These findings indicate that all fractions of PT exhibit potent •OH radical scavenging activity.

NADH phosphate oxidase, a membrane-bound enzyme that reduces free molecular oxygen by one electron, generates O₂⁻ radicals (Chun et al., 2003). These O₂⁻ radicals can further produce additional ROS, such as •OH radicals and H₂O₂, leading to oxidative damage in the body (Benov, 2001; Chung and Jeon, 2011). Table 3 presents the O₂⁻ radical scavenging activity of the EtOH extract and four PT fractions. Furthermore, only the EtOH extract and EtOAc fraction of PT exhibited more than 20% radical scavenging activity at a concentration of 100 µg/mL. While the scavenging activity of the EtOH extracts and EtOAc fractions was relatively high, their overall O₂⁻ scavenging activity was lower compared to the scavenging activities observed for other radicals such as DPPH, ABTS⁺, and •OH.

In other studies on PT, Kwon et al. (2020) reported higher radical scavenging activity in assessments of DPPH and O₂⁻ radical scavenging (with IC₅₀ values for DPPH, •OH, and O₂⁻ of the EtOAc fraction at 8.21, 1.06, and 39.99 µg/mL, respectively). Despite being the same plant species, variations in radical scavenging activity can arise owing to differences in results depending on plant origin, cultivation environment, and experimental conditions. However, our overall results of radical scavenging activities showed a similar trend, with the EtOAc fraction also demonstrating the highest radical scavenging activity. Therefore, our findings indicate that

TABLE 4 Radical scavenging activities of active compounds 1–3 from PT.

Scavenging activity	Concentration ($\mu\text{g/mL}$)	Compound (%)		
		Salicin (1)	Salireposide (2)	Populin (3)
DPPH radical	1	-	-	4.42 ± 1.73^b
	2.5	-	7.99 ± 2.60^c	6.22 ± 1.75^b
	5	0.66 ± 0.99^b	15.68 ± 0.88^b	9.27 ± 0.70^a
	10	4.87 ± 1.89^a	22.63 ± 1.59^a	2.21 ± 1.95^c
	IC ₅₀ (mM)	25.30 ± 12.36	0.33 ± 0.06	-
ABTS ⁺ radical	1	-	6.08 ± 0.44^d	0.03 ± 1.58^b
	2.5	-	10.82 ± 0.85^c	1.53 ± 2.01^{ab}
	5	1.78 ± 1.30^b	18.66 ± 0.62^b	2.36 ± 2.48^{ab}
	10	5.35 ± 3.03^a	29.72 ± 1.19^a	3.02 ± 2.71^a
	IC ₅₀ (mM)	13.54 ± 4.26	0.19 ± 0.01	-
•OH radical	1	20.82 ± 2.21^d	26.86 ± 1.00^d	15.41 ± 2.22^d
	2.5	39.12 ± 0.77^c	39.48 ± 1.46^c	28.32 ± 2.94^c
	5	49.21 ± 2.21^b	44.34 ± 1.00^b	42.29 ± 2.51^b
	10	53.00 ± 1.42^a	51.78 ± 0.79^a	50.90 ± 1.62^a
	IC ₅₀ (mM)	0.02 ± 0.00	0.02 ± 0.00	0.02 ± 0.00
O ₂ ⁻ radical	1	5.22 ± 1.06^d	13.62 ± 2.03^d	16.82 ± 1.53^c
	2.5	18.33 ± 1.10^c	19.89 ± 3.45^c	25.77 ± 4.68^b
	5	27.98 ± 1.64^b	32.52 ± 4.58^b	27.91 ± 4.84^b
	10	33.76 ± 2.04^a	37.12 ± 1.59^a	37.52 ± 4.24^a
	IC ₅₀ (mM)	0.11 ± 0.01	0.07 ± 0.01	0.12 ± 0.05

Values are means \pm SD.

^{a-d}Means are significantly different ($p < 0.05$) by Duncan's multiple range test. IC₅₀ is the concentration in $\mu\text{g/mL}$ required to inhibit the formation of radicals by 50%.

the EtOH extract and four fractions of PT possess radical scavenging activity *in vitro*, scavenging DPPH, ABTS⁺, •OH, and O₂⁻ radicals. Particularly, the EtOAc fraction exhibited the strongest radical scavenging activity among the extract and other fractions, highlighting it as a potent fraction of PT.

Three compounds such as salicin (1), salireposide (2), and populin (3), were isolated from the EtOAc PT fraction, and their structures were identified (Figure 1). Table 4 presents the DPPH, ABTS⁺, •OH, and O₂⁻ radical scavenging activities of the isolated compounds from the EtOAc fractions of PT, which were evaluated to assess their chemical profiles. Most radical scavenging activities showed concentration-dependent behavior. Among these three compounds, salireposide (2) exhibited the lowest IC₅₀ value of 0.33 ± 0.06 , 0.19 ± 0.01 , 0.02 ± 0.00 , and 0.07 ± 0.01 mM for DPPH, ABTS⁺, •OH, and O₂⁻ radical scavenging activity, respectively. Salireposide (2) exhibited the highest scavenging activities among all radical scavenging activities experiments, except for •OH radical scavenging activity. It is reasonable to infer that salireposide (2) plays a significant role in contributing to the high radical scavenging ability of the EtOAc fraction of PT.

In the context of structure-activity relationships, hydroxyl groups typically donate hydrogen atoms and stabilizing free

radicals. Hydroxyl groups in the *ortho* or *para* positions (not *meta*) enhance radical scavenging activity by stabilizing the resulting phenoxyl radical through resonance. Compounds including salicin, salireposide, and populin, which form intramolecular hydrogen bonds, exhibit heightened radical scavenging activity owing to phenoxyl radical stabilization (Tirado-Kulieva et al., 2022; Spiegel et al., 2020). Furthermore, glycosylation of phenolic compounds seems to increase their radical scavenging activities potential, possibly by enhancing bioavailability and serving as prodrugs that release more bioactive aglycones *in vivo* upon hydrolysis (Johnson et al., 2021; Zhang et al., 2006). Therefore, this structural characteristic of salicin (1), salireposide (2), and populin (3) significantly contributes to the observed high radical scavenging activity in the EtOAc fraction.

3.4 Cytotoxicity of PT extracts and fractions on RAW264.7 cells

To compare the effect of the PT extract and its fractions on the viability of RAW264.7 cells, an MTT assay was performed (Figure 3A). The viability of RAW264.7 cells treated with the PT

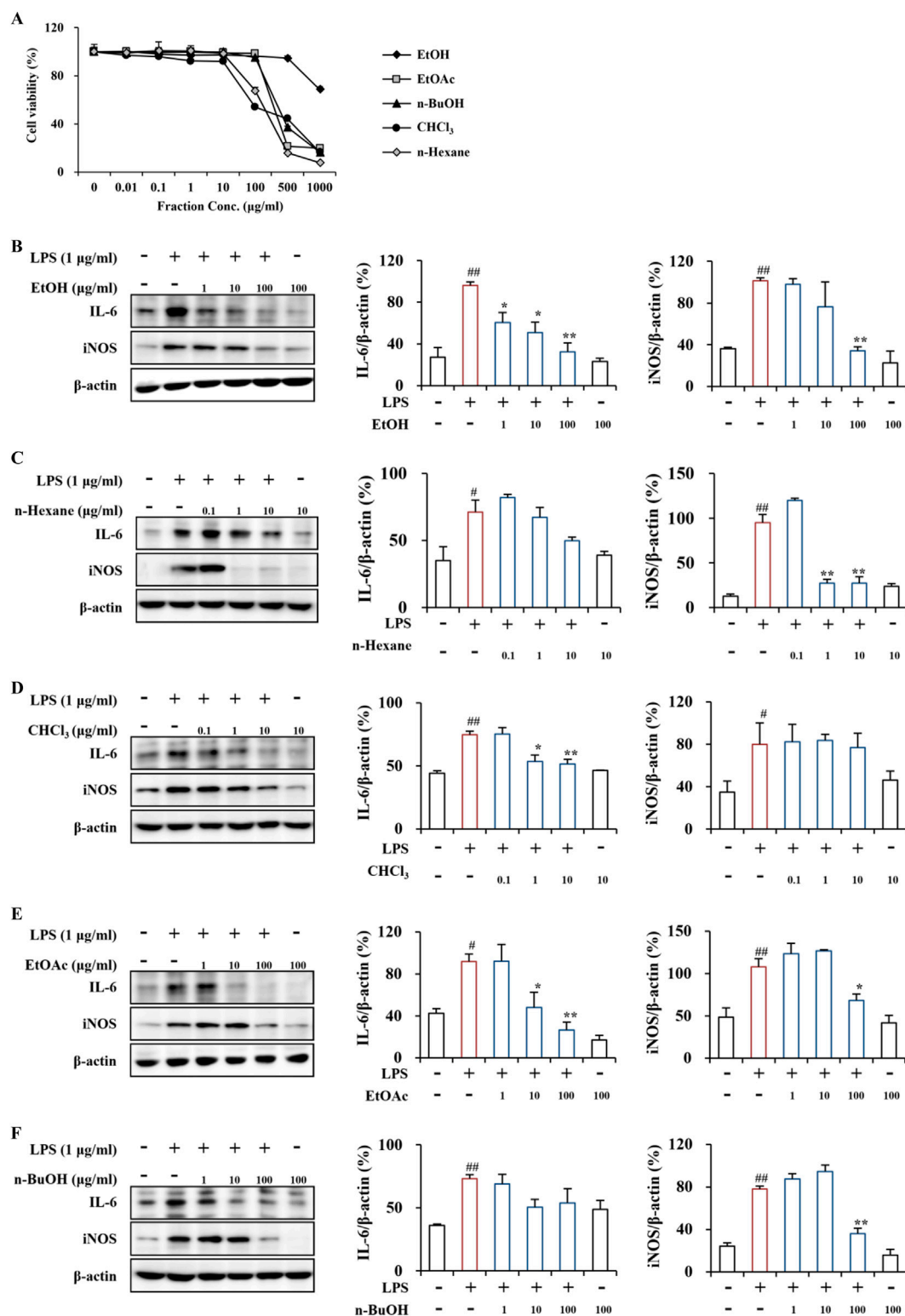


FIGURE 3 Cytotoxicity and anti-inflammatory effects of PT extract and its fractions on RAW264.7 cells. (A) Cytotoxicity of the PT extract and its fractions on RAW264.7 cells. RAW264.7 cells were treated with the PT extract and its four fractions (EtOH, *n*-hexane, CHCl₃, EtOAc, and *n*-BuOH solvents), and cell viability was assessed using an MTT assay. (B–F) Anti-inflammatory effects of the PT extract and its fractions on LPS-induced RAW264.7 cells. LPS-induced RAW264.7 cells were pretreated with the PT extract and its four fractions using EtOH (B), *n*-hexane (C), CHCl₃ (D), EtOAc (E), and *n*-BuOH (F) solvents. The cell lysates (*n* = 3 per group) from all groups were analyzed by Western blot analysis using IL-6 and iNOS antibodies (B–F), representing the inflammatory cytokine and enzyme, respectively. The results were quantified (B–F), and data are presented as the mean expressive value (the ratio of each value against GAPDH for each sample) ± SEM (one-way ANOVA with *post hoc* test; ^{##}*p* < 0.01 compared to the Control group, ^{*}*p* < 0.05 and ^{**}*p* < 0.01 compared to the LPS-induced group).

extract and its four fractions did not significantly differ from the vehicle control (DMSO) at concentrations of 0.01–500 µg/mL for the EtOH extract, 0.01–100 µg/mL for the EtOAc and *n*-BuOH fractions, and 0.01–10 µg/mL for the *n*-hexane and CHCl₃ fractions (Figure 3A). These results suggest that the PT extract and its fractions do not exhibit specific cell toxicity at concentrations below 500, 100, or 10 µg/mL.

3.5 Anti-inflammatory effects of PT extracts and its fractions in LPS-induced RAW264.7 cells

In the LPS-induced RAW264.7 cells, the EtOH extract clearly reduced the protein expression of the representative proinflammatory cytokine IL-6 at concentrations of 1–100 µg/mL and the enzyme iNOS at 100 µg/mL (Figure 3B). The *n*-hexane fraction did not significantly influence IL-6 expression at concentrations of 0.1–10 µg/mL; however, effectively decreased iNOS protein expression at concentration of 1 and 10 µg/mL (Figure 3C). The CHCl₃ fraction significantly downregulated IL-6 protein expression at concentration of 1 and 10 µg/mL; however, did not influence iNOS protein expression at concentrations of 0.1–10 µg/mL (Figure 3D). The EtOAc fraction significantly reduced the protein expression of IL-6 and iNOS at the concentration of 10 and 100 and 100 µg/mL, respectively (Figure 3E). The *n*-BuOH fraction did not significantly affect the protein expression of IL-6 and iNOS at concentrations of 1–100 µg/mL; however, it markedly down-regulated iNOS expression at 100 µg/mL (Figure 3F). Additionally, the EtOH extract and four fractions of PT demonstrated anti-inflammatory activity by inhibiting the protein expression of the representative pro-inflammatory cytokine IL-6 and the enzyme iNOS in the LPS-induced RAW264.7 macrophages (Figure 3). The anti-inflammatory activity of the EtOH extract and EtOAc fraction was superior to that of other fractions (Figure 3). A recent study reported that pretreatment with PT extract mitigated neuronal loss by alleviating glial activation (an indicator of neuroinflammation) in the gerbil hippocampal CA1 area caused by transient global cerebral ischemia (Park et al., 2017). Neuroinflammation, a characteristic feature of neurological disorders, primarily results from chronically activated glial cells (astrocytes and microglia) in the pathological lesion (Kwon and Koh, 2020). Activated glia produces various proinflammatory cytokines, including IL-6 and IL-1β, and enzymes such as iNOS and cyclooxygenase-2 (Kwon and Koh, 2020). Thus, blocking glial activity may be a novel approach to regulating various neurological disorders (Kwon and Koh, 2020). Since non-neurological disorders, including autoimmune and chronic diseases, also involve inflammatory reactions (Laveti et al., 2013), further exploration of PT is necessary to understand its physiological and pathological activities.

4 Conclusion

Nine phenolic compounds were isolated from the PT leaves, including novel butyl ester derivatives of luteolin and chrysoeriol,

which have not been previously described in the Salicaceae family. The EtOH extract and its fractions showed potent and dose-dependent radical scavenging and anti-inflammatory activities against DPPH, ABTS⁺, hydroxyl radicals, superoxide anions, IL-6, and iNOS. The EtOAc fraction demonstrated superior activity in most assays compared to the extract and other fractions. While salireposide (2) demonstrated significant radical scavenging activities capabilities, attributing the efficacy of PT solely to this compound would be premature. The observed bioactivities likely result from the synergistic interaction of various phytochemicals within PT. This study emphasizes the anti-inflammatory potential of PT, suggesting its potential as a valuable source of natural bioactive metabolites for developing functional food and therapeutic agents.

Data availability statement

The original contributions presented in the study are included in the article/supplementary material, further inquiries can be directed to the corresponding authors.

Author contributions

H-DL: Investigation, Methodology, Validation, Visualization, Writing–original draft. JiK: Investigation, Methodology, Visualization, Writing–original draft. JC: Investigation, Methodology, Writing–original draft. KK: Supervision, Visualization, Writing–review and editing. JaK: Conceptualization, Supervision, Writing–review and editing. KC: Data curation, Supervision, Writing–review and editing. HK: Conceptualization, Supervision, Writing–review and editing. SL: Conceptualization, Funding acquisition, Supervision, Writing–review and editing. I-HC: Conceptualization, Funding acquisition, Supervision, Writing–review and editing.

Funding

The author(s) declare that financial support was received for the research, authorship, and/or publication of this article. This research was supported by grants from the National Institute of Biological Resources (NIBR), funded by the Ministry of Environment (MOE) (NIBR202134206), and the National Research Foundation of Korea (NRF), funded by the Ministry of Science and ICT (NRF-2022R1A2C2009817), Republic of Korea.

Conflict of interest

The authors declare that the research was conducted in the absence of any commercial or financial relationships that could be construed as a potential conflict of interest.

The author(s) declared that they were an editorial board member of *Frontiers*, at the time of submission. This had no impact on the peer review process and the final decision.

Publisher's note

All claims expressed in this article are solely those of the authors and do not necessarily represent those of their affiliated

organizations, or those of the publisher, the editors and the reviewers. Any product that may be evaluated in this article, or claim that may be made by its manufacturer, is not guaranteed or endorsed by the publisher.

References

- Abreu, I. N., Ahnlund, M., Moritz, T., and Albrechtsen, B. R. (2011). UHPLC-ESI/TOFMS determination of salicylate-like phenolic glycosides in *Populus tremula* leaves. *J. Chem. Ecol.* 37, 857–870. doi:10.1007/s10886-011-9991-7
- Ahmad, V. U., Abbasi, M. A., Hussain, H., Akhtar, M. N., Farooq, U., Fatima, N., et al. (2003). Phenolic glycosides from *Symplocos racemosa*: natural inhibitors of phosphodiesterase I. *Phytochemistry* 63, 217–220. doi:10.1016/s0031-9422(03)00075-x
- Akbari-Ahangar, A., and Delnavazi, M. R. (2020). Flavone glycosides from the aerial parts of *Stachys lavandulifolia* Vahl. *Pharm. Sci.* 26, 198–202. doi:10.34172/ps.2020.4
- Andelković, B., Vujišić, L., Vučković, I., Tešević, V., Vajs, V., and Godevac, D. (2017). Metabolomics study of *Populus* type propolis. *J. Pharm. Biomed. Anal.* 135, 217–226. doi:10.1016/j.jpba.2016.12.003
- Ashenhurst, J. (2022). D and L notation for sugars. *Master Org. Chem.* Available at: <https://www.masterorganicchemistry.com/2017/05/24/d-and-l-sugars/> (Accessed September 18, 2022).
- Benov, L. (2001). How superoxide radical damages the cell. *Protoplasma* 217, 33–36. doi:10.1007/bf01289410
- Brown, M. J. (2016). *Synthetic vs natural nutrients: does it matter?* Healthline. Available at: <https://www.healthline.com/nutrition/synthetic-vs-natural-nutrients> (Accessed August 17, 2016).
- Choi, J. H., Oh, J., Lee, M. J., Bae, H., Ko, S. G., Nah, S. Y., et al. (2021a). Inhibition of lysophosphatidic acid receptor 1–3 deteriorates experimental autoimmune encephalomyelitis by inducing oxidative stress. *J. Neuroinflammation* 18, 240–320. doi:10.1186/s12974-021-02278-w
- Choi, J. H., Oh, J., Lee, M. J., Ko, S. G., Nah, S. Y., and Cho, I. H. (2021b). Gintonin mitigates experimental autoimmune encephalomyelitis by stabilization of Nrf2 signaling via stimulation of lysophosphatidic acid receptors. *Brain Behav. Immun.* 93, 384–398. doi:10.1016/j.bbi.2020.12.004
- Choi, S. I., Hwang, S. J., Lee, O. H., and Kim, J. D. (2020). Antioxidant activity and component analysis of *Populus tomentiglandulosa* extract. *Korean J. Food Sci. Technol.* 52, 119–124. doi:10.9721/kjfst.2020.52.119
- Chun, O. K., Kim, D. O., and Lee, C. Y. (2003). Superoxide radical scavenging activity of the major polyphenols in fresh plums. *J. Agric. Food Chem.* 51, 8067–8072. doi:10.1021/jf034740d
- Chung, G. Y., Chang, K. S., Chung, J.-M., Choi, H. J., Paik, W.-K., and Hyun, J.-O. (2017). A checklist of endemic plants on the Korean Peninsula. *Korean J. Pl. Taxon.* 47, 264–288. doi:10.11110/kjpt.2017.47.3.264
- Chung, H.-J., and Jeon, I.-S. (2011). Antioxidative activities of methanol extracts from different parts of *Chrysanthemum zawadskii*. *Korean J. Food preserv.* 18, 739–745. doi:10.11002/kjfp.2011.18.5.739
- Debbache-Benaïda, N., Atmani-Kilani, D., Schini-Keirith, V. B., Djebbi, N., and Atmani, D. (2013). Pharmacological potential of *Populus nigra* extract as antioxidant, anti-inflammatory, cardiovascular and hepatoprotective agent. *Asian pac. J. Trop. Biomed.* 3, 697–704. doi:10.1016/s2221-1691(13)60141-0
- Di Domenico, F., Barone, E., Perluigi, M., and Butterfield, D. A. (2014). Strategy to reduce free radical species in Alzheimer's disease: an update of selected antioxidants. *Expert Rev. Neurother.* 15, 19–40. doi:10.1586/14737175.2015.955853
- Gondor, O. K., Pál, M., Janda, T., and Szalai, G. (2022). The role of methyl salicylate in plant growth under stress conditions. *J. Plant. Physiol.* 277, 153809. doi:10.1016/j.jplph.2022.153809
- Greenwood Resources (2014). Hybrid poplar and the pulp and paper industry in North America: implications for a secured supply of quality fiber for papermakers worldwide. Available at: <https://link.springer.com/article/10.1http://greenwoodresources.com/wp-content/uploads/2014/09/hybrid-poplar-white-paper.pdf>;S1022795416100069 (Accessed December 22, 2015).
- Guleria, I., Kumari, A., Lacaille-Dubois, M. A., Kumar, V., Saini, A. K., Lal, S., et al. (2021). A review on the genus *Populus*: a potential source of biologically active compounds. *Phytochem. Rev.* 21, 987–1046. doi:10.1007/s11101-021-09772-2
- Habib, H. M., and Ibrahim, W. H. (2011). Effect of date seeds on oxidative damage and antioxidant status in vivo. *J. Sci. Food Agric.* 91, 1674–1679. doi:10.1002/jsfa.4368
- Harbilas, D., Brault, A., Vallerand, D., Martineau, L. C., Saleem, A., Arnason, J. T., et al. (2012). *Populus balsamifera* L. (Salicaceae) mitigates the development of obesity and improves insulin sensitivity in a diet-induced obese mouse model. *J. Ethnopharmacol.* 141, 1012–1020. doi:10.1016/j.jep.2012.03.046
- Hernández-Rodríguez, P., Baquero, L. P., and Larrota, H. R. (2019). "Flavonoids: potential therapeutic agents by their antioxidant capacity," in *Bioactive compounds: health benefits and potential applications*. Editor M. R. S. Campos (Woodhead Publishing, Sawston), 265–288. doi:10.1016/B978-0-12-814774-0.00014-1
- Ilhan, M., Ali, Z., Khan, I. A., Taştan, H., and Akkol, E. K. (2019). Bioactivity-guided isolation of flavonoids from *Urtica dioica* L. and their effect on endometriosis rat model. *J. Ethnopharmacol.* 243, 112100. doi:10.1016/j.jep.2019.112100
- Jadid, N., Hidayati, D., Hartanti, S. R., Arraniry, B. A., Rachman, R. Y., and Wikanta, W. (2017). "Antioxidant activities of different solvent extracts of *Piper retrofractum* Vahl. using DPPH assay," in *AIP conference proceedings* (New York, USA: American Institute of Physics). 020019–020025. doi:10.1063/1.4985410
- Jang, M., Choi, J. H., Chang, Y., Lee, S. J., Nah, S. Y., and Cho, I. H. (2019). Gintonin, a ginseng-derived ingredient, as a novel therapeutic strategy for Huntington's disease: activation of the Nrf2 pathway through lysophosphatidic acid receptors. *Brain Behav. Immun.* 80, 146–162. doi:10.1016/j.bbi.2019.03.001
- Johnson, J. B., Mani, J. S., Broszczak, D., Prasad, S. S., Ekanayake, C. P., Strappe, P., et al. (2021). Hitting the sweet spot: a systematic review of the bioactivity and health benefits of phenolic glycosides from medicinally used plants. *Phytother. Res.* 35, 3484–3508. doi:10.1002/ptr.7042
- Kedare, S. B., and Singh, R. P. (2011). Genesis and development of DPPH method of antioxidant assay. *J. Food Sci. Technol.* 48, 412–422. doi:10.1007/s13197-011-0251-1
- Khan, M. I. R., Fatma, M., Per, T. S., Anjum, N. A., and Khan, N. A. (2015). Salicylic acid-induced abiotic stress tolerance and underlying mechanisms in plants. *Front. Plant. Sci.* 6, 462. doi:10.3389/fpls.2015.00462
- Kosseva, M. R., and Webb, C. (2013). *Food industry wastes: assessment and recuperation of commodities*. (Cambridge: Academic Press). doi:10.1016/b978-0-12-391921-2.00028-7
- Krishnaiah, D., Sarbatly, R., and Nithyanandam, R. (2011). A review of the antioxidant potential of medicinal plant species. *Food. Bioprod. process.* 89, 217–233. doi:10.1016/j.fbp.2010.04.008
- Kumari, A., Upadhyay, N. K., and Khosla, P. K. (2016). Gender specific variation of two phenolic glycosides (Populin and salicin) in *Populus ciliata* and identification of a new compound (cinnamoyl-salicin). *Int. J. Pharm. Pharm. Sci.* 8, 156–162. doi:10.22159/ijpps.2016v8i12.14843
- Kwon, H. S., and Koh, S. H. (2020). Neuroinflammation in neurodegenerative disorders: the roles of microglia and astrocytes. *Transl. Neurodegener.* 9, 42–12. doi:10.1186/s40035-020-00221-2
- Kwon, Y. R., Kim, J. H., Lee, S., Cho, E. J., and Kim, H. Y. (2020). Protective role of *Populus tomentiglandulosa* against hydrogen peroxide-induced oxidative stress in SH-SY5Y neuronal cells. *J. Appl. Biol. Chem.* 63, 357–363. doi:10.3839/jabc.2020.047
- Laveti, D., Kumar, M., Hemalatha, R., Sistla, R., Naidu, V. G. M., Talla, V., et al. (2013). Anti-inflammatory treatments for chronic diseases: a review. *Inflamm. Allergy Drug Targets* 12, 349–361. doi:10.2174/18715281113129990053
- Lee, C. H., Park, J. H., Ahn, J. H., Kim, J. D., Cho, J. H., Lee, T. K., et al. (2019a). Stronger antioxidant enzyme immunoreactivity of *Populus tomentiglandulosa* extract than ascorbic acid in rat liver and kidney. *Iran. J. Basic Med. Sci.* 22, 963–967. doi:10.22038/ijbms.2019.34926.8296
- Lee, M. J., Choi, J. H., Oh, J., Lee, Y. H., In, J. G., Chang, B. J., et al. (2021a). Rg3-enriched Korean Red Ginseng extract inhibits blood-brain barrier disruption in an animal model of multiple sclerosis by modulating expression of NADPH oxidase 2 and 4. *J. Ginseng Res.* 45, 433–441. doi:10.1016/j.jgr.2020.09.001
- Lee, S.-S., Kim, H.-G., Park, E.-H., Kim, K.-J., Bang, M.-H., Kim, G., et al. (2021b). Antioxidant and anti-inflammatory effects in lipopolysaccharide-induced THP-1 cells of coumarins from the bark of *Hesperethusa crenulata* R. *Appl. Biol. Chem.* 64, 90. doi:10.1186/s13765-021-00665-8
- Lee, T. K., Park, J. H., Ahn, J. H., Kim, H., Song, M., Lee, J. C., et al. (2019b). Pretreatment of *Populus tomentiglandulosa* protects hippocampal CA1 pyramidal neurons from ischemia-reperfusion injury in gerbils via increasing SODs expressions and maintaining BDNF and IGF-I expressions. *Chin. J. Nat. Med.* 17, 424–434. doi:10.1016/S1875-5364(19)30050-0
- Li, X. (2013). Solvent effects and improvements in the deoxyribose degradation assay for hydroxyl radical-scavenging. *Food Chem.* 141 (3), 2083–2088. doi:10.1016/j.foodchem.2013.05.084
- Lipinski, B. (2011). Hydroxyl radical and its scavengers in health and disease. *Oxid. Med. Cell. Longev.* 2011, 809696. doi:10.1155/2011/809696

- Liu, H., Wu, H., Wang, Y., Wang, F., Liu, X., and Zhou, Z. (2021). Enhancement on antioxidant and antibacterial activities of Brightwell blueberry by extraction and purification. *Appl. Biol. Chem.* 64, 78. doi:10.1186/s13765-021-00649-8
- Liu, S. C., Lin, J. T., Hu, C. C., Shen, B. Y., Chen, T. Y., Chang, Y. L., et al. (2017). Phenolic compositions and antioxidant attributes of leaves and stems from three inbred varieties of *Lycium chinense* Miller harvested at various times. *Food Chem.* 215, 284–291. doi:10.1016/j.foodchem.2016.06.072
- Lu, S., Ahmed, S. A., and Chong, S.-H. (2006). Micro structural changes in juvenile and matured wood of *Populus tomentiglandulosa* T. J. *Korea Furnit. Soc.* 17, 29–36.
- Lyngsie, G., Krumina, L., Tunlid, A., and Persson, P. (2018). Generation of hydroxyl radicals from reactions between a dimethoxyhydroquinone and iron oxide nanoparticles. *Sci. Rep.* 8, 10834. doi:10.1038/s41598-018-29075-5
- Mahdi, J. G., Mahdi, A. J., Mahdi, A. J., and Bowen, I. D. (2006). The historical analysis of aspirin discovery, its relation to the willow tree and antiproliferative and anticancer potential. *Cell. Prolif.* 39, 147–155. doi:10.1111/j.1365-2184.2006.00377.x
- Martemucci, G., Costagliola, C., Mariano, M., D'andrea, L., Napolitano, P., and D'Alessandro, A. G. (2022). Free radical properties, source and targets, antioxidant consumption and health. *Oxygen* 2, 48–78. doi:10.3390/oxygen2020006
- Morreel, K., Goeminne, G., Storme, V., Sterck, L., Ralph, J., Coppieters, W., et al. (2006). Genetical metabolomics of flavonoid biosynthesis in *Populus*: a case study. *Plant J.* 47, 224–237. doi:10.1111/j.1365-3113.2006.02786.x
- Nam, J. S., Park, S. Y., Jang, H. L., and Rhee, Y. H. (2017). Phenolic compounds in different parts of young *Annona muricata* cultivated in Korea and their antioxidant activity. *Appl. Biol. Chem.* 60, 535–543. doi:10.1007/s13765-017-0309-5
- Nzowa, L. K., Barboni, L., Teponno, R. B., Ricciuti, M., Lupidi, G., Quassinti, L., et al. (2010). Rheediosides A and B, two antiproliferative and antioxidant triterpene saponins from *Entada rheedii*. *Phytochemistry* 71, 254–261. doi:10.1016/j.phytochem.2009.10.004
- Park, J. H., Lee, T. K., Ahn, J. H., Shin, B. N., Cho, J. H., Kim, I. H., et al. (2017). Pretreated *Populus tomentiglandulosa* extract inhibits neuronal loss and alleviates gliosis in the gerbil hippocampal CA1 area induced by transient global cerebral ischemia. *Anat. Cell Biol.* 50, 284–292. doi:10.51115/acb.2017.50.4.284
- Phaniendra, A., Jestadi, D. B., and Periyasamy, L. (2015). Free radicals: properties, sources, targets, and their implication in various diseases. *Indian J. Clin. Biochem.* 30, 11–26. doi:10.1007/s12291-014-0446-0
- Pizzino, G., Irrera, N., Cucinotta, M., Pallio, G., Mannino, F., Arcoraci, V., et al. (2017). Oxidative stress: harms and benefits for human health. *Oxid. Med. Cell. Longev.* 2017, 8416763. doi:10.1155/2017/8416763
- Sharma, O. P., and Bhat, T. K. (2009). DPPH antioxidant assay revisited. *Food. Chem.* 113, 1202–1205. doi:10.1016/j.foodchem.2008.08.008
- Shi-hui, Q. (2012). Studies on chemical constituents of *Lycopus lucidus* Turcz. var. *hirtus* Regel. *Chin. J. Exp. Tradit. Med. Formulae* 18, 83–85.
- Shojaefard, Z., Hemmateenejad, B., and Jassbi, A. R. (2021). Chemometrics-based LC-UV-ESIMS analyses of 50 *Salvia* species for detecting their antioxidant constituents. *J. Pharm. Biomed. Anal.* 193, 113745. doi:10.1016/j.jpba.2020.113745
- Simard, F., Legault, J., Lavoie, S., and Pichette, A. (2014). Balsacones DI, dihydrocinnamoyl flavans from *Populus balsamifera* buds. *Phytochemistry* 100, 141–149. doi:10.1016/j.phytochem.2013.12.018
- Son, Y. (2009). From science area to politic area; development and distribution of Eunsuwonsasi tree. *The Korean J. Hist. Sci.* 31, 437–474.
- Spiegel, M., Kapusta, K., Kołodziejczyk, W., Saloni, J., Żbikowska, B., Hill, G. A., et al. (2020). Antioxidant activity of selected phenolic acids–ferric reducing antioxidant power assay and QSAR analysis of the structural features. *Molecules* 25, 3088. doi:10.3390/molecules25133088
- Thaipong, K., Boonprakob, U., Crosby, K., Cisneros-Zevallos, L., and Byrne, D. H. (2006). Comparison of ABTS, DPPH, FRAP, and ORAC assays for estimating antioxidant activity from guava fruit extracts. *J. Food Compos. Anal.* 19, 669–675. doi:10.1016/j.jfca.2006.01.003
- Tirado-Kulieva, V. A., Hernández-Martínez, E., and Choque-Rivera, T. J. (2022). Phenolic compounds versus SARS-CoV-2: an update on the main findings against COVID-19. *Heliyon* 8, e10702. doi:10.1016/j.heliyon.2022.e10702
- Tsai, C. J., Harding, S. A., Tschaplinski, T. J., Lindroth, R. L., and Yuan, Y. (2006). Genome-wide analysis of the structural genes regulating defense phenylpropanoid metabolism in *Populus*. *New Phytol.* 172, 47–62. doi:10.1111/j.1469-8137.2006.01798.x
- Vidya, B., Palaniswamy, M., Sowmya, S., Priyanga, S., Perumal, P. C., Devaki, R., et al. (2016). Evaluate the antioxidant activity and FT-IR spectroscopic analysis of purified β -galactosidase from *Aspergillus terreus*. *Indoam. J. Pharm.* 6, 6383–6392.
- Wei, J. H., Xi, Q. N., Zeng, Y. T., Li, B., Li, Y., Qian, X. Y., et al. (2018). Flavonoids of Zhuang medicine *Cardiospermum halicacabum*. *Zhong Cao Yao* 49, 2502–2507. doi:10.7501/j.issn.0253-2670.2018.11.003
- Xu, L., Liu, H., Ma, Y., Wu, C., Li, R., and Chao, Z. (2018). Isomeric phenolic glycosides from *Populus tomentosa*. *Rec. Nat. Prod.* 13, 97–103. doi:10.25135/rnp.82.18.03.257
- Yang, Y., Chen, M., Zhang, W., Zhu, H., Li, H., Niu, X., et al. (2023). Metabolome combined with transcriptome profiling reveals the dynamic changes in flavonoids in red and green leaves of *Populus euramericana* 'Zhonghuahongye'. *Front. Plant Sci.* 14, 1274700. doi:10.3389/fpls.2023.1274700
- Zeng, Q. H., Zhang, X. W., Xu, X. L., Jiang, M. H., Xu, K. P., Piao, J. H., et al. (2013). Antioxidant and anticomplement functions of flavonoids extracted from *Penthorum chinense* Pursh. *Food Funct.* 4, 1811–1818. doi:10.1039/c3fo60342c
- Zhang, X. F., Thuong, P. T., Min, B. S., Ngoc, T. M., Hung, T. M., Lee, I. S., et al. (2006). Phenolic glycosides with antioxidant activity from the stem bark of *Populus davidiana*. *J. Nat. Prod.* 69, 1370–1373. doi:10.1021/np060237u